Title

Fuzzy modeling approach for transient vapor compression and expansion cycle simulation

Authors

Kim, Donghun
Ma, Jiacheng
Braun, James E
et al.

Publication Date

2021

DOI

10.1016/j.ijrefrig.2020.10.025

Peer reviewed

Journal Pre-proof

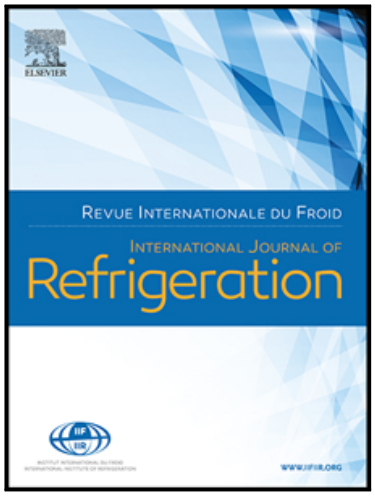

Fuzzy Modeling Approach for Transient Vapor Compression and Expansion Cycle Simulation

Donghun Kim, Jiacheng Ma, James E. Braun, Eckhard A. Groll

PII: S0140-7007(20)30435-7
DOI: https://doi.org/10.1016/j.ijrefrig.2020.10.025
Reference: JIJR 4937

To appear in: *International Journal of Refrigeration*

Received date: 1 April 2020
Revised date: 21 October 2020
Accepted date: 22 October 2020

Please cite this article as: Donghun Kim, Jiacheng Ma, James E. Braun, Eckhard A. Groll, Fuzzy Modeling Approach for Transient Vapor Compression and Expansion Cycle Simulation, *International Journal of Refrigeration* (2020), doi: https://doi.org/10.1016/j.ijrefrig.2020.10.025

Fuzzy Modeling Approach for Transient Vapor Compression and Expansion Cycle Simulation

Donghun Kim[a,b,*], Jiacheng Ma[a], James E. Braun[a], Eckhard A. Groll[a]

[a] *School of Mechanical Engineering, Purdue University, West Lafayette, IN, USA*
[b] *Energy Technologies Area, Building Technology & Urban Systems Division, Lawrence Berkeley National Laboratory, CA, USA*

Abstract

Previous mode switching algorithms for heat exchanger moving boundary models in the literature are composed of a set of IF-THEN rules. These representations could lead to numerical challenges due to the inherited discontinuities associated with IF-THEN rules. This paper presents an alternative mode switching methodology which results in a continuous moving boundary heat exchanger model over all possible mode changes. Numerical performance of the proposed method for a heat exchanger has been tested using simulations and sample results are compared with a moving boundary model with switching based on IF-THEN rules and also a finite-volume method. The proposed switching algorithm was implemented within a complete vapor compression cycle model and results were compared with experimental data for a start-up transient.

Keywords: moving boundary, switching algorithm, transient heat exchanger simulation, fuzzy modeling

Nomenclature

Symbols

χ^*	Extended quality [-]
$\dot{m}$	Mass flow rate [kg s^{-1}]
$\dot{Q}$	Heat transfer rate [kW]
A	Refrigerant Flow Area [m^2]
adj	Adjoint matrix

*Corresponding author
Email address: donghunkim@lbl.gov (Donghun Kim)

det	Determinant
E	Coefficient matrix
F	Fuzzy rules
h	Specific enthalpy [kJ kg^{-1}]
L	Heat exchanger length [m]
m	Shaping parameter [-]
P	Pressure [kPa]
T	Temperature [C]
u	Input
x	Dynamic states
z	Normalized zone length [-]
LP	Large Positive
N	Negative
P	Positive
SC	Subcool
SCTP	Subcool - two phase
SCTPSH	Subcool - two phase - superheat
SH	Superheat
SHTP	Superheat - two phase
SHTPSC	Superheat - two phase - subcool
TP	Two phase
TPSC	Two phase - subcool
TPSH	Two phase - superheat
Z	Zero

Greek letters

ϵ	Shaping parameter [-]
μ	Membership functions
ω	Weight functions

ρ	Density [kg m^{-3}]

Subscript

cond	Condenser
e	Exit
env	Secondary fluid
evap	Evaporator
f	Saturated liquid
i	Inlet
j	Zone index
t	Tube
v	Saturated vapor
w	Water

1. Introduction

Transient modeling of systems that incorporate thermodynamic cycles, e.g. vapor compression cycles (VCC) and organic rankine cycles (ORC), provides a way of evaluating and designing controllers to efficiently and reliably operate those systems. Since the dynamics of heat exchangers have the greatest effect on the overall transient behavior of VCC and ORC systems, developing an accurate but computationally fast heat exchanger model is an important step. The finite volume method (FVM) and moving boundary method (MB) are popular approaches for dynamic heat exchanger modeling (Bendapudi, Braun and Groll, 2008). While the FVM divides heat exchangers into a number of fixed control volumes, the MB segments heat exchanges depending on thermodynamic phase of the refrigerant, i.e. subcooled liquid (SC), two phase (TP) and superheated vapor (SH), and moves control volumes as the length of each phase changes. Consequently, the MB solves fewer equations due to fewer control volumes. Because of the lower state dimensionality and a reasonable accuracy of the MB (Bendapudi et al., 2008; Li and Alleyne, 2010; McKinley and Alleyne, 2008; Rasmussen and Alleyne, 2004), the MB has been extensively utilized for many control applications for VCC and ORC systems (Galindo, Dolz, Royo-Pascual, Haller and Melis, 2016; Pettit, Willatzen and Ploug-Sørensen, 1998; Shi, He, Peng, Zhang and Zhuge, 2016; Wei, Lu, Lu and Gu, 2008).

Since the phase zones could appear or disappear inside of a heat exchanger depending on operating conditions, and MB formulations depend on those phase modes, a MB model generally consists of case-by-case mathematical descriptions and a switching algorithm to decide which description should be used.

MB formulations have been derived and advanced in a series of papers. Grald and MacArthur (1992) developed a two-zone MB formulation for an evaporator (TPSH), and incorporated a void fraction model for the TP region. A comparison with a FVM model demonstrated accuracy of the MB model with a lower computational cost. He, Liu, Asada and Itoh (1998) explored MB models for both condenser and evaporator. The evaporator dynamics were lumped into two zones (TPSH), and the condenser dynamics into three zones (SHTPSC). The model was proven to be useful for a feedback control design. Pettit et al. (1998) formulated a set of heat exchanger MB models for SCTPSH, SCTP, TP and TPSH modes for an evaporator. A switching algorithm that monitors enthalpy and selects an appropriate mode was presented. Munch Jensen and Tummescheit (2002) tested a virtually identical three-zone moving boundary model for an evaporator (SCTPSH) for an ORC. Zhang and Zhang (2006) investigated the MB evaporator model employing a time variant void fraction model. The model was able to switch between TP and TPSH modes when the superheated region length was used to trigger switch events. Bendapudi et al. (2008) extended the MB formulations for more general phase combinations, e.g. SH, SHTP and SHTPSC for condenser and TP and TPSH for evaporator, and applied the enthalpy based IF-THEN rules for mode switching. The main challenge within the model structures is in the mismatch of the number of state dimensions for different modes. McKinley and Alleyne (2008) provided a method that can systematically overcome the mismatch problem by introducing pseudo-state variables. In the methodology, dynamic states associated with inactive zones are evaluated by pseudo state equations when a phase zone disappears. This provides a reasonable initial condition for the states when a zone appears.

Despite a long history and a large number of investigations and applications of the MB method, there is still a significant challenge in designing a general and reliable switching algorithm for smooth transitions between the case-by-case model representations. As mentioned in Bendapudi et al. (2008), the MB formulation is less robust and more sensitive to a shape of boundary conditions compared with the FVM when a heat exchanger undergoes several mode switches during a very short time period, e.g. start-up. Pangborn, Alleyne and Wu (2015) also showed that the FVM performs better in terms of stability and robustness although the MB approach can execute much faster and achieve similar levels of accuracy with the FVM for most cases except for large transients. It has also been pointed out that developing switching criteria for a smooth transition between modes is significantly challenging for the MB. To improve the MB to overcome those numerical issues, Several studies have focused on the development of a reliable and general switching algorithm Bendapudi et al. (2008); Li and Alleyne (2010); Pangborn et al. (2015); Pettit et al. (1998); Qiao, Laughman, Aute and Radermacher (2016); Qiao et al. (2016); Rasmussen and Shenoy (2012); Rodriguez and Rasmussen (2017).

However, all approaches are based on IF-THEN rules, and hence contain potential numerical issues due to inherent discontinuities of IF-THEN rules. This paper provides an alternative mode switching algorithm that can overcome this

issue and that can cover all possible modes and mode changes in a consistent and intuitive way. It does not contain any IF-THEN rules in the algorithm and eliminates discontinuities even at singular points of MB HX formulations. A simulation case study result, where numerical issues of a IF-THEN rule based MB model appear but not for the proposed model, is provided first. Model validation with available experimental data for a start-up transient VCC is presented to demonstrate the capability of the switching scheme between multiple mode changes.

2. Potential issues of IT-THEN model and research motivation

For a several decades, numerical integration algorithms have been evolved to handle discontinuities of functions or their derivatives. Pioneered by Cellier (1979), a typical algorithm treating discontinuities includes four steps: 1) detect whether there are discontinuities within a time step with zero-cross function(s), 2) when a state event is triggered, locate where the discontinuity happens within a threshold, 3) run an integration solver until the left hand side of the location (defined by the threshold), and 4) pass over the location, reset and restart the integration. This technique provides a sound numerical method and have been embedded in many simulation solvers or software packages such as Simulink (Zhang, Yeddanapudi and Mosterman, 2008) and Modelica Dymola (Brück, Elmqvist, Mattsson and Olsson, 2002). However, there are still a variety of theoretical and numerical reasons for not favoring discontinuous models of ordinary differential equations (ODE) or differential algebraic systems of equations (DAE). Well-known issues of simulating discontinuous ODE or DAE models are;

- It is required that ODE or DAE models be continuously differentiable for some degrees to have a local error estimate and continuous numerical integration, since most numerical integration methods are based on this assumption (Bradie, 2006; Dahlquist, Björck et al., 1974).
- When events are triggered, numerical algorithms for handling discontinuities halt the integration and restart the simulation (see the fourth step above) typically with a very short time step because the discontinuities could cause fast changes in some state variables requiring a small step to stay within the allowed error tolerance. (Cellier and Kofman, 2006; Lundvall, Fritzson and Bachmann, 2008).
- The numerical approach in face of discontinuity could become prohibitively expensive for a large scale model (Casella, 2015). For example, consider a chiller plant model which consists of a chiller, cooling tower, pumps, valves, and cooling coil models. Suppose a state-event is triggered in the chiller model (e.g., due to the appearance or reappearance of thermal zone). Then, a solver starts an iteration process to identify the location of the discontinuity not only with the chiller model but with the entire system model! We refer to Casella (2015) for more detailed discussions.

- It is possible that numerical algorithms for handling discontinuities may fail to detect a discontinuity. An example includes when there are an even number of zero crosses within a time step (chosen by an adaptive time step solver). In this case, the underlying zero-crossing detection algorithm can miss them (since the sign of the product of two boundary values of a zero-cross function will be positive).

- Chattering could occur (Mosterman, 1999). The simulation of a bouncing ball where a discontinuity occurs whenever the ball hits the ground is one of the simplest example of the chattering and *Zeno* phenomenon.

- The property of the continuous differentiability with respect to all state variables is one of conditions to establish the existence and uniqueness of a solution to the differential equation (Coddington and Levinson, 1955). Differentiability is also needed because model equations are differentiated during translation to reduce the index of the DAE system if it is higher than one, and to compute the Jacobian matrix. In addition, boundness of the derivative is needed to avoid situations where the step size of Newton-based solvers for nonlinear equations shrinks to zero Wetter, Zuo, Nouidui and Pang (2014).

Those issues have driven simulation research communities, the Modelica Association (https://www.modelica.org/) in particular, to reformulate a variety of event generating functions such as IF-THEN based models to smooth them. Examples include Modelica Buildings Library (Wetter et al., 2014), OpenModelica (Fritzson, Aronsson, Pop, Lundvall, Nystrom, Saldamli, Broman and Sandholm, 2006; Lundvall et al., 2008) and ThermoCycle (Quoilin, Desideri, Wronski, Bell and Lemort, 2014). All reformulation approaches adopt some kinds of transition functions to smooth or filter the discontinuities embedded in event generating functions.

3. Notations and brief descriptions of MB mode switching problem

A MB formulation for a HX depends on thermodynamic phase zones of a refrigerant. In this paper, MB formulations for shell-and-tube heat exchangers from Bendapudi et al. (2008) are adopted and summarized in Kim (2019). Each mode which is a combination of SC, TP and SH has a final form of $\mathbf{E}_j(x)\dot{x} = \mathbf{f}_j(x,u)$ or $\dot{x} = F_j(x,u)$ where $F_j = \mathbf{E}_j^{-1}(x)\mathbf{f}_j(x,u)$ for each mode number $j \in \{1,\cdots,6\}$. Those equations were formulated to have consistent dynamic state x and input u which are defined as

$$x = [P, h_e, z_1, z_2, T_{t1}, T_{t2}, T_{t3}, T_{w1}, T_{w2}, T_{w3}]^T \quad (1)$$

$$u = [\dot{m}_i, \dot{m}_e, h_i, \dot{m}_{wi}, T_{wi}]^T. \quad (2)$$

The pseudo-state methodology proposed by McKinley and Alleyne (2008) is adopted for this purpose when a phase zone is inactive. The zone numbers of 1, 2, 3 are defined by the refrigerant flow direction. For evaporators, they

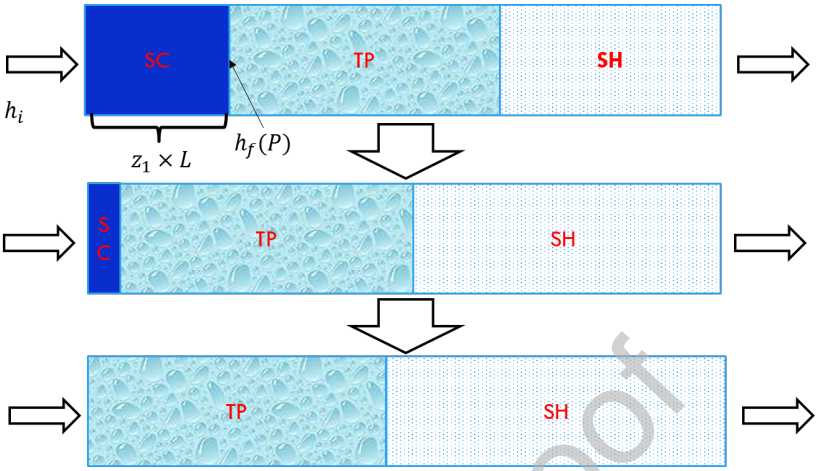

Figure 1: An example of mode switching from SCTPSH to TPSH

mean subcooling liquid (SC), two-phase (TP), and superheated vapor (SH), respectively. On the other hand, they are SH, TP and SC for condensers.

It is worthwhile to mention that the typical moving boundary formulation, previous MB papers in the literature and this paper focus on pure refrigerants. The applicability of the moving boundary formulation for mixtures is still a research topic; See Kim, Ziviani, Braun and Groll (2017) for an issue of applying the moving boundary heat exchanger model for a binary mixture.

When a heat exchanger experiences changes of operating conditions, such as heat load and refrigerant flow rate, a new thermodynamic phase zone may appear and disappear. Fig. 1 shows a conceptual example of a mode change where the subcooling liquid zone disappears as the inlet enthalpy h_i increases. In this case, corresponding equations need to be switched from the three-zone mode to the two-zone mood. A fundamental question of designing a mode switching algorithm is when to switch from a mode to another.

Within a HX, there are many possible mode and mode changes as shown in Fig. 2. This implies many event detection rules need to be designed. Double arrows in the figure indicate that a switching rule may be directionally dependent. For example, a rule from TPSH to SCTPSH could differ to that from SCTPSH to TPSH.

Obviously, the goal of switching algorithm design is to develop rules which are generally applicable to cover all mode changing scenarios in a numerically reliable and efficient manner.

One important characteristic of the algorithm design problem is the singularity associated with a mode change. See Willatzen, Pettit and Ploug-Sørensen (1998) for the singularity problem in numerics during a mode change. Mathematically, it is related to the fact that $det(\mathbf{E}_j(x)) \to 0$ as a zone appears or disappears which makes $F_j(x, u)$ unbounded at singular points.

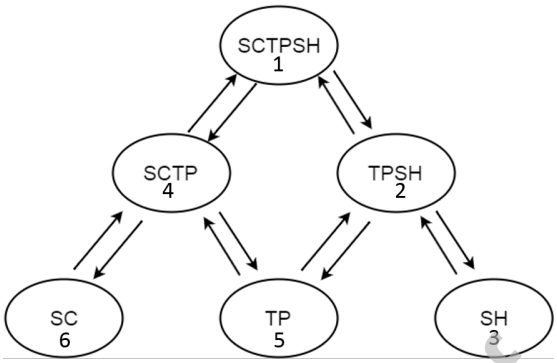

Figure 2: Possible mode and mode changes in a evaporator

As mentioned, all switching algorithms in the literature rely on a set of IF-THEN rules may have potential issues listed in Section 2 and that have complex representations due to the number of mode changing scenarios.

4. Alternative switching algorithm: an example

Objectives of our switching algorithm design are 1) to allow transitions between all possible HX modes shown in Fig. 2, and 2) to avoid IF-THEN rules which bring additional numerical challenges, e.g. chattering and increased stiffness.

We illustrate our methodology for an evaporator using the simple case depicted in Fig. 1, then present a generalized HX model in the following section. Our main tool to achieve those goals is a fuzzy modeling approach, so called Takagi-Sugeno (TS) fuzzy modeling (Takagi and Sugeno, 1985). The idea of the TS fuzzy modeling is quite simple but powerful when we want to create a systematic interpolation from multiple sub-functions that are valid on their own subdomains. A step by step procedure of applying the fuzzy modeling approach to the HX MB mode switching problem is described as follows.

4.1. Defining fuzzy variable

We define the following variable.

$$\chi^* := \frac{h - h_f(P)}{h_v(P) - h_f(P)}, \quad \forall h \in \mathbb{R}. \tag{3}$$

Note that χ^* is a generalized version of the quality. It is the quality when $h \in [h_f, h_v]$, but could be either negative or larger than unity outside of this range. χ^*, namely extended quality, will be an indicator for selecting or fusing a set of fuzzy rules. We denote χ_i^* for the extended quality at the inlet of a HX, i.e. $\chi_i^* := \chi^*(h_i, P)$.

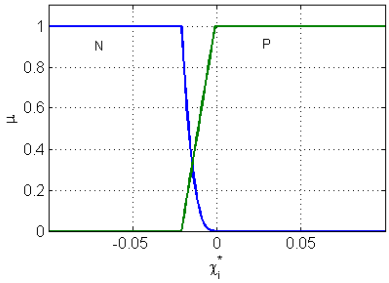

Figure 3: Membership functions of N,P for χ_i^* ($\epsilon = 1/50, m = 3$)

4.2. Defining linguistic values and membership functions

Let us define two linguistic values of N and P for χ_i^*, where N denotes negative and P is positive. A membership function for each linguistic value was designed as follow.

$$\mu_N(\chi_i^*) = \begin{cases} 1 & (\chi_i^* < -\epsilon) \\ (-\frac{\chi_i^*}{\epsilon})^m & (-\epsilon \le \chi_i^* < 0) \\ 0 & (0 \le \chi_i^*) \end{cases} \tag{4}$$

$$\mu_P(\chi_i^*) = \begin{cases} 0 & (\chi_i^* < -\epsilon) \\ \frac{\chi_i^*}{\epsilon} + 1 & (-\epsilon \le \chi_i^* < 0) \\ 1 & (0 \le \chi_i^*) \end{cases} \tag{5}$$

ϵ and m are parameters that define the shapes of the membership functions. The functions with $\epsilon = 1/50, m = 3$ are depicted in Fig. 3. A more detailed description for shapes of membership functions are discussed in a later section.

4.3. Design of fuzzy rules

We use the following fuzzy rules for switching between the two models of SCTPSH and TPSH.

R1: If χ_i^* is N, then $\dot{x} = F_1(x, u)$.

R2: If χ_i^* is P, then $\dot{x} = F_2(x, u)$.

Refer to Eqn. (25) in Kim (2019) for the definitions of F_1, F_2. These rules could be interpreted as "When the inlet condition is liquid, then use the SCTPSH model. When the inlet condition is two phase, then use the TPSH model". The set of rules is basically a fuzzy version of the switching rules of Bendapudi et al. (2008); Pettit et al. (1998) which are

If $h_i < h_f$, then $\dot{x} = F_1(x, u)$,

If $h_i \ge h_f$, then $\dot{x} = F_2(x, u)$.

4.4. Defuzzification and fuzzy model

Using a standard fuzzy inference approach, we construct the final fuzzy system model as follows.

$$\dot{x} = F(x, u) \tag{6}$$

where

$$F(x,u) = \omega_1(\chi_i^*) \times \tilde{F}_1(x,u) + \omega_2(\chi_i^*) \times \tilde{F}_2(x,u) \tag{7}$$

$$\omega_1(\chi_i^*) = \frac{\mu_N(\chi_i^*)}{\mu_N(\chi_i^*) + \mu_P(\chi_i^*)} \tag{8}$$

$$\omega_2(\chi_i^*) = \frac{\mu_P(\chi_i^*)}{\mu_N(\chi_i^*) + \mu_P(\chi_i^*)} \tag{9}$$

where $\tilde{F}_j$ is an extended function of F_j which will be discussed later. At this moment, treat $\tilde{F}_j = F_j$.

Let's consider a behavior of the fuzzy model of Eqn. (6). When χ_i^* is sufficiently small ($\chi_i^* < -\epsilon$), F is identical to F_1 because $\mu_N(\chi_i^*) = 1$ and $\mu_P(\chi_i^*) = 0$ (see Eqn. (4)). Likewise, $F = F_2$ when χ_i^* is sufficiently positive. Within the region of $(-\epsilon, 0)$, F transforms between F_1 and F_2 according to weight functions of $w_1(\cdot)$ and $w_2(\cdot)$. The membership functions play roles of deciding the weights depending on the value of χ_i^*. Generally speaking, the value of F at a point (in an appropriate vector space) is a convex combination of values of F_1 and F_2 because $\omega_1(\chi_i^*) + \omega_2(\chi_i^*) = 1$ and $\omega_1(\chi_i^*) \geq 0, \omega_1(\chi_i^*) \geq 0$ for all $\chi_i^* \in \mathbb{R}$. This means the value of F lies on the line segment between the values of F_1 and F_2 in an appropriate vector space and hence bounded by them. A conceptual plot of the TS-fuzzy model is shown in Fig. 4.

There are some generic characteristics of the proposed MB model. First, see that 1) IF-THEN rules of **R1** and **R2** disappeared through the process of the fuzzy inference, and 2) the final model of Eqn. (6) has a standard ode form. Therefore the fuzzy model is more robust for controller design and analysis than any other IF-THEN rule-based MB models. Second, note that the way of constructing the fuzzy model is systematic and straightforward: one only needs to come up with heuristic rules for mode changes, e.g. **R1** and **R2**, and design membership functions. Then, a well developed fuzzy inference method automatically defuzzifies the set of rules and casts a final form. As shown in the next section, this feature allows developing a general MB fuzzy model that can cover all possible mode change scenarios in a straightforward manner.

A couple of points should be addressed to have desired numerical properties of the final fuzzy model F. First, to utilize the TS-fuzzy modeling, it is necessary to have F_1 and F_2 defined on a common transition domain as depicted in Fig. 4. However, in MB formulations, those functions are defined on their own domains that are possibly disjointed. For example, the domain of F_1 for the SCTPSH mode is confined by $h_i < h_f(P)$, meanwhile that of F_2 for the TPSH mode

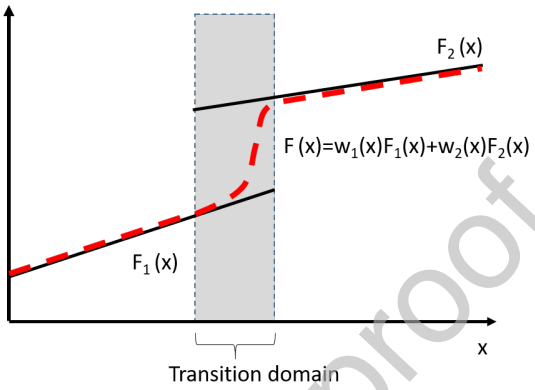

Figure 4: Conceptual plot of a result of fuzzy reasoning

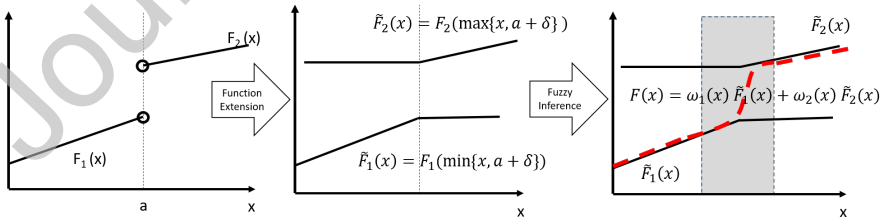

Figure 5: Conceptual diagram of applying the fuzzy modeling to MB problems

is restricted by $h_f(P) < h_i$. To handle this problem, we introduce extended functions of F_1 and F_2 for this example case, say $\tilde{F}_1$ and $\tilde{F}_2$, as follows.

$$\tilde{F}_1(\cdots, h_i, \cdots) = F_1(\cdots, min\{h_i, h_f(P) - \delta\}, \cdots) \tag{10}$$

$$\tilde{F}_2(\cdots, h_i, \cdots) = F_2(\cdots, max\{h_i, h_f(P) + \delta\}, \cdots) \tag{11}$$

The max and min processes are to extend function values outside the function domains by mapping h_i into the domains. Other domain constraints, e.g. $0 < z_{SC}$ and $h_i < h_e$ can be treated in the same manner to define a generalized extended function. We do not provide complete expressions for the general extended functions, because it is very long to list all equations due to a number of variables and different domain restrictions that are dependent on modes. However, one can easily construct them by capping variables with domain bounds: Those functions have either max or min expressions on variables of h_i, h_e, z_1, z_2, z_3 depending on modes. When we refer to $\tilde{F}_j$, it is the extension of F_j considering all domain restrictions associated with the j^{th} mode.

Note that, through this extension, $\tilde{F}_1$ and $\tilde{F}_2$ are defined everywhere so that there is a common domain. δ is an arbitrarily small positive number, e.g. 10^{-5}, which is introduced to treat the *open* set nature of the domains and to make the extended functions bounded even at the singular points associated with $h_i = h_f(P)$, e.g. $z_{SC} = 0$.

It is important to note that $\tilde{F}_1$ and $\tilde{F}_2$ are continuous everywhere. This is because F_1 and F_2 are continuous on their own domains, the operations of max and min are continuous everywhere, and the corresponding images are subsets of the domains. In addition, it can be shown that ω_j are continuous everywhere. These imply the fuzzy MB model of Eqn. (6) is continuous everywhere which makes it more reliable than IF-THEN rule-based MB models since it avoids discontinuities during mode switches. Fig. 5 summarizes the conceptual work flow.

It is also important to mention that the singularity issue of F_1 when the SC zone disappears, i.e. $det(E_1(x)) \to 0$, could be naturally handled with δ and the weight function associated with F_1. For example, consider when $h_i \to h_f^-$. This describes the subcooled zone length decreasing to 0, and makes $det(\mathbf{E}_1(x)) \to 0$. However, due to the capping action of δ, $\tilde{F}_1(x, u)$ would be bounded ($< \infty$). In addition, $w_1(\chi_i^*) \to 0$ since $\chi_i^* \to 0^-$ implies $\mu_N(\chi_i^*) \to 0$ and $\mu_P(\chi_i^*) \to 1$ (see Fig. 3). This shows the value of the term of $w_1(\chi_i^*) \times \tilde{F}_1(x, u) \to 0$ during the mode switch. The parameter m for the design of membership functions (see Eqn. (4)) should bring the term to 0 more efficiently and make F less stiff. In this paper, $m = 3$ was selected for the membership functions based on a parametric study.

5. Development of a general switching algorithm

Consider general mode change scenarios shown in Fig. 2. We will develop a general MB fuzzy model through the same procedure discussed in the preceding section.

5.1. Defining fuzzy variable

Five fuzzy variables (non-dimensional) are defined: χ_i^*, χ_e^*, z_{SC}, z_{TP}, z_{SH}. The first two are extended qualities associated with h_i and h_e (See Eqn. (3)), and the rest are scaled zone lengths for SC, TP and SH zones. The reason for choosing those variables is due to a design of fuzzy rules that will be described later.

5.2. Defining linguistic values and membership functions

For each χ_i^* and χ_e^*, we define three linguistic values of N, P and LP where N denotes negative, P is positive and LP means large positive. Corresponding 6 membership functions are designed as follows.

$$\mu_{i,N}(\chi_i^*) = \begin{cases} 1 & (\chi_i^* < -\epsilon) \\ (-\frac{\chi_i^*}{\epsilon})^m & (-\epsilon \le \chi_i^* < 0) \\ 0 & (0 \le \chi_i^*) \end{cases} \tag{12}$$

$$\mu_{i,P}(\chi_i^*) = \begin{cases} 0 & (\chi_i^* < -\epsilon) \\ \frac{\chi_i^*}{\epsilon} + 1 & (-\epsilon \le \chi_i^* < 0) \\ 1 & (0 \le \chi_i^* < 1-\epsilon) \\ (-\frac{(\chi_i^*-1)}{\epsilon})^m & (1-\epsilon \le \chi_i^* < 1) \\ 0 & (1 \le \chi_i^*) \end{cases} \tag{13}$$

$$\mu_{i,LP}(\chi_i^*) = \begin{cases} 0 & (\chi_i^* < 1-\epsilon) \\ \frac{\chi_i^*-1}{\epsilon} + 1 & (1-\epsilon \le \chi_i^* < 1) \\ 1 & (1 \le \chi_i^*) \end{cases} \tag{14}$$

$$\mu_{e,N}(\chi_e^*) = \begin{cases} 1 & (\chi_e^* < -\epsilon) \\ (-\frac{\chi_e^*}{\epsilon})^m & (-\epsilon \le \chi_e^* < 0) \\ 0 & (0 \le \chi_i^*) \end{cases} \tag{15}$$

$$\mu_{e,P}(\chi_e^*) = \begin{cases} 0 & (\chi_e^* < 0) \\ (\frac{\chi_e^*}{\epsilon})^m & (0 \le \chi_e^* < \epsilon) \\ 1 & (\epsilon \le \chi_i^* < 1) \\ 1 - \frac{\chi_e^*-1}{\epsilon} & (1 \le \chi_e^* < 1+\epsilon) \\ 0 & (1+\epsilon \le \chi_e^*) \end{cases} \tag{16}$$

$$\mu_{e,LP}(\chi_e^*) = \begin{cases} 0 & (\chi_e^* < 1) \\ (\frac{\chi_e^*-1}{\epsilon})^m & (1 \le \chi_e^* < 1+\epsilon) \\ 1 & (1+\epsilon \le \chi_e^*) \end{cases} \tag{17}$$

ϵ and m are parameters shaping the membership functions. Membership functions with ($\epsilon = 1/50, m = 3$) are depicted in Fig. 6.

For fuzzy variables of z_{SC}, z_{TP}, z_{SH}, two linguistic values of Z and P are defined where Z is zero and P means positive. The corresponding membership functions are

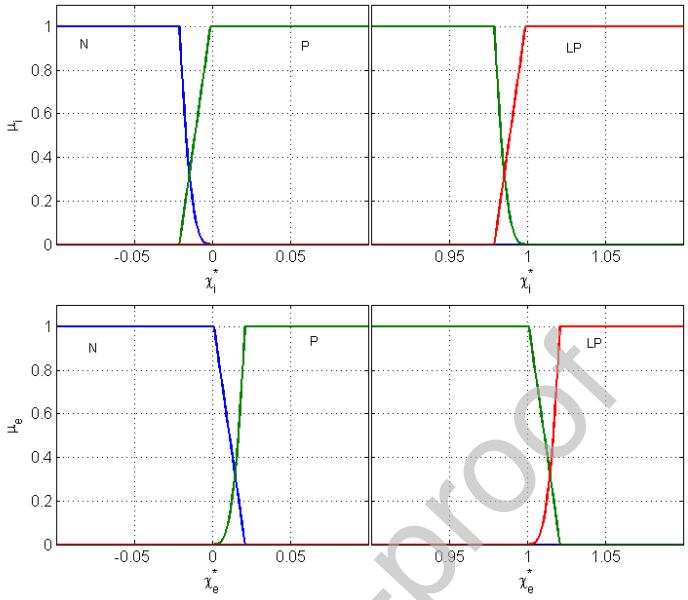

Figure 6: Membership functions for N,P and LP for χ_i^* and χ_e^* ($\epsilon = 1/50, m = 3$)

$$\mu_Z(z) = \begin{cases} 1 - (\frac{z}{\epsilon})^m & (0 \le z < \delta + \epsilon) \\ 0 & (\epsilon \le z) \end{cases} \tag{18}$$

$$\mu_P(z) = \begin{cases} (\frac{z}{\epsilon})^m & (0 \le z < \epsilon) \\ 1 & (\epsilon \le z) \end{cases} \tag{19}$$

Membership functions with ($\epsilon = 1/100, m = 4$) are depicted in Fig. 7.

The selection of a membership function and corresponding parameters, e.g., ϵ and m, influences the behavior of the fuzzy system. That is, it depends on how the designer intends to tune the entire fuzzy system and is still a subjective, application-dependent and open research topic. For example, note that the parameters for the extended qualities and scaled zone lengths proposed in this Section are inconsistent. They were chosen based on parametric studies by looking at the trade-off between accuracy and computational cost of the final fuzzy model.

5.3. Design of fuzzy rules

We chose the following rules for evaporator and condenser cases.

Evaporator

R1: If (χ_i^* is N and χ_e^* is LP) or (z_{SC} is P and z_{TP} is P and z_{SH} is P), then $\dot{x} = F_1(x, u)$

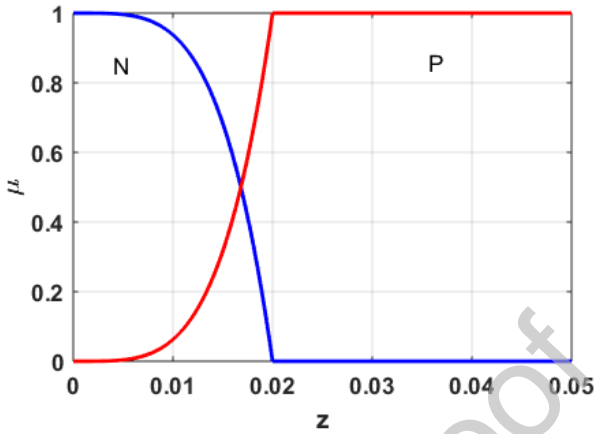

Figure 7: Membership function of Z and P for z_{SC}, z_{TP}, z_{SH}, $(\epsilon = 1/100, m = 4)$

R2: If (χ_i^* is P and χ_e^* is LP) or (z_{SC} is Z and z_{TP} is P and z_{SH} is P), then $\dot{x} = F_2(x, u)$

R3: If (χ_i^* is LP and χ_e^* is LP) or (z_{SC} is Z and z_{TP} is Z and z_{SH} is P), then $\dot{x} = F_3(x, u)$

R4: If (χ_i^* is N and χ_e^* is P) or (z_{SC} is P and z_{TP} is P and z_{SH} is Z), then $\dot{x} = F_4(x, u)$

R5: If (χ_i^* is P and χ_e^* is P) or (z_{SC} is Z and z_{TP} is P and z_{SH} is Z), then $\dot{x} = F_5(x, u)$

R6: If (χ_i^* is N and χ_e^* is N) or (z_{SC} is P and z_{TP} is Z and z_{SH} is Z), then $\dot{x} = F_6(x, u)$

Condensor

R1: If (χ_i^* is LP and χ_e^* is N) or (z_{SC} is P and z_{TP} is P and z_{SH} is P), then $\dot{x} = F_1(x, u)$

R2: If (χ_i^* is LP and χ_e^* is P) or (z_{SC} is Z and z_{TP} is P and z_{SH} is P), then $\dot{x} = F_2(x, u)$

R3: If (χ_i^* is LP and χ_e^* is LP) or (z_{SC} is Z and z_{TP} is Z and z_{SH} is P), then $\dot{x} = F_3(x, u)$

R4: If (χ_i^* is P and χ_e^* is N) or (z_{SC} is P and z_{TP} is P and z_{SH} is Z), then $\dot{x} = F_4(x, u)$

R5: If (χ_i^* is P and χ_e^* is P) or (z_{SC} is Z and z_{TP} is P and z_{SH} is Z), then $\dot{x} = F_5(x, u)$

R6: If (χ_i^* is N and χ_e^* is N) or (z_{SC} is P and z_{TP} is Z and z_{SH} is Z), then $\dot{x} = F_6(x, u)$

The rules have very intuitive physical meanings. For example, **R1** for evaporator refers to "when the inlet phase is liquid (inlet quality is negative) and exit phase is vapor (exit quality is large positive) or when all lengths for liquid, two-phase and vapor phase zones are positive, use the SCTPSH model".

5.4. Defuzzification and fuzzy model

Adopting a standard fuzzy inference approach results in the final fuzzy model.

$$\dot{x} = F(x,u) \tag{20}$$

$$= \frac{\sum_{j=1}^{6} \mu_j \times \tilde{F}_j(x,u)}{\sum_{j=1}^{6} \mu_j} \tag{21}$$

$$= \sum_{j=1}^{6} \omega_j \times \tilde{F}_j(x,u), \tag{22}$$

where $\omega_j = \mu_j / \sum_{k=1}^{6} \mu_k$ and μ_j is the maximum between the products of membership functions for χ_i^* and χ_e^* associated with the j^{th} rule and that of membership functions for z_{SC}, z_{TP}, z_{SH} associated with the rule. For example, μ_1 for an evaporator is

$$\mu_1 = max\{\mu_{i,N}(\chi_i^*) \times \mu_{e,P}(\chi_e^*), \mu_P(z_{SC}) \times \mu_P(z_{TP}) \times \mu_P(z_{SH})\}, \tag{23}$$

μ_2 for an evaporator is

$$\mu_2 = max\{\mu_{i,P}(\chi_i^*) \times \mu_{e,LP}(\chi_e^*), \mu_Z(z_{SC}) \times \mu_P(z_{TP}) \times \mu_P(z_{SH})\}. \tag{24}$$

The operations of multiplication and maximum between membership functions are results of a defuzzification process for "AND" and "OR" logic. Intuitively, the max operation chooses a weight for a rule based on the *certainty* of enthalpy criteria or that of length criteria, whichever is greater.

It can be shown that $0 \leq \omega_j \leq 1 \; \forall j \in \{1, \cdots, 6\}$, and $\sum_j^6 \omega_j = 1$. Therefore the fuzzy model can be regarded as a weighted average of the set of local models of $\dot{x} = \tilde{F}_j(x, u)$, and the value of $\tilde{F}$ at a point is bounded by values of the local models as discussed.

Besides the desired numerical features discussed in the previous Section 5.4, it is surprising to see how systematically the fuzzy modeling approach eliminates IF-THEN rules, and how compactly it represents a MB model that can cover a variety of mode change scenarios. Remember that almost all approaches of IF-THEN rule-based MB switching algorithms in the literature developed for general scenarios are very complex. This is because ways of detecting disappearing and appearing zones are different, i.e. directionally dependent, for each

mode change. For example, the mode change from SCTPSH to TPSH could be detected by tracking the liquid zone length and comparing it with a user specified threshold. However for the opposite case, an alternative scheme must be used, because the liquid zone length is useless for TPSH to trigger the SCTPSH mode. The final form of Eqn. (20) is more useful for application to control-oriented problems than other IF-THEN based MB models.

6. Numerical test under multiple mode changes

A numerical experiment following the approach of Pettit et al. (1998) was carried out where a HX experiences multiple mode transitions from SHTPSC to SHTP, TP and TPSC sequentially. Perturbation profiles of boundary conditions to shift the HX mode from SHTPSC to SHTP, TP, TPSC and SHTPSC were based on Pettit et al. (1998) and are shown in Fig. 8. The condensing pressure was fixed during the entire simulation period of 600 sec according to the reference paper. Initial and boundary conditions are summarized in Table 1.

A shell-and-tube water cooled condenser was considered in this test. For detailed descriptions of the heat exchanger and heat transfer correlations for the refrigerant and water, refer to Bendapudi et al. (2008). The proposed MB switching algorithm with the MB HX formulations were implemented using Simulink version R2017b. An adaptive time step ode solver, ode15s, which is suitable for stiff systems (Shampine and Reichelt, 1997) was used. A detailed FVM model was simulated to provide a baseline. In this test, the fuzzy model was also compared with a IF-THEN mode switching scheme. The IF-THEN rules used here are similar to those in Bendapudi et al. (2008); Pettit et al. (1998); Rodriguez and Rasmussen (2017): disappearance of a zone is detected by comparing a zone length with a user-specified threshold. For example, it switches from SHTPSC to SHTP if $z_L \leq L_\epsilon$ where L_ϵ is a user-specified parameter. On the other hand, appearance of a zone is detected by comparing the HX inlet or outlet enthalpy with a saturated enthalpy. For example, the condenser switches from TP to SHTP when the inlet enthalpy is above the saturated vapor enthalpy, and switches from SHTP to SHTPSC when the outlet enthalpy is below the saturated liquid enthalpy. An enthalpy threshold (Bonilla, Dormido and Cellier, 2015) defined below is used.

$$\frac{h_f - h_e}{h_f} < h_\epsilon \tag{25}$$

In this test, normalized length and enthalpy thresholds were both set to 0.01.

The results are presented in Fig. 9. Exit enthalpy results demonstrate the accuracy of the fuzzy model by comparing the prediction with that of the FVM model. From the inlet and outlet enthaply profiles together with saturated liquid and vapor enthalpies (straight dashed lines), it is clear that the mode shifts from SHTPSC to TPSH, TP, TPSC and SHTPSC: The HX mode changed from SHTPSC to SHTP at around 50 sec, when the refrigerant inlet mass flow rate increased. Since the input enthalpy moved below the saturated vapor enthalpy

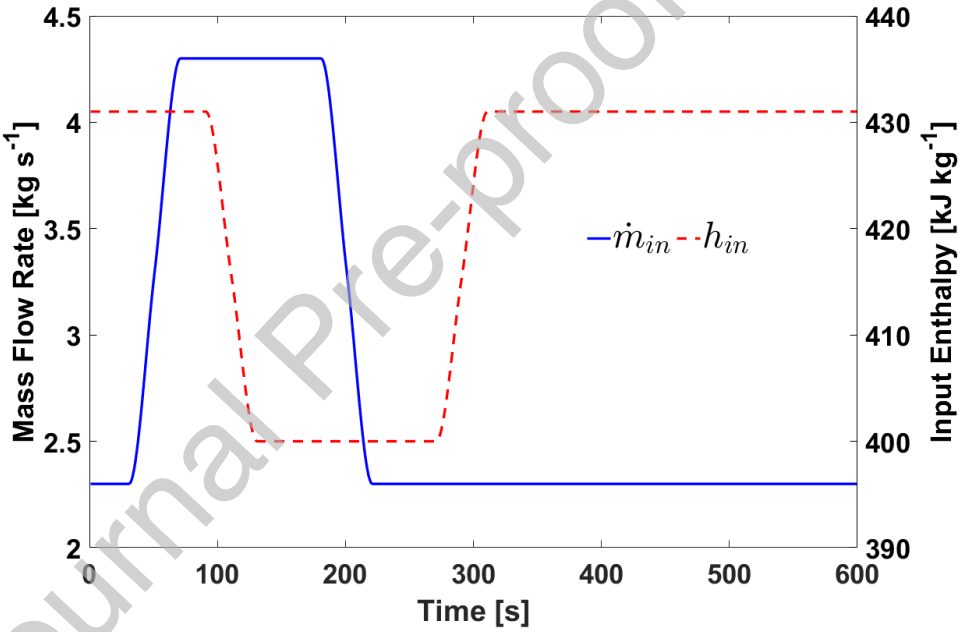

Figure 8: Refrigerant inlet mass flow rate and inlet enthalpy

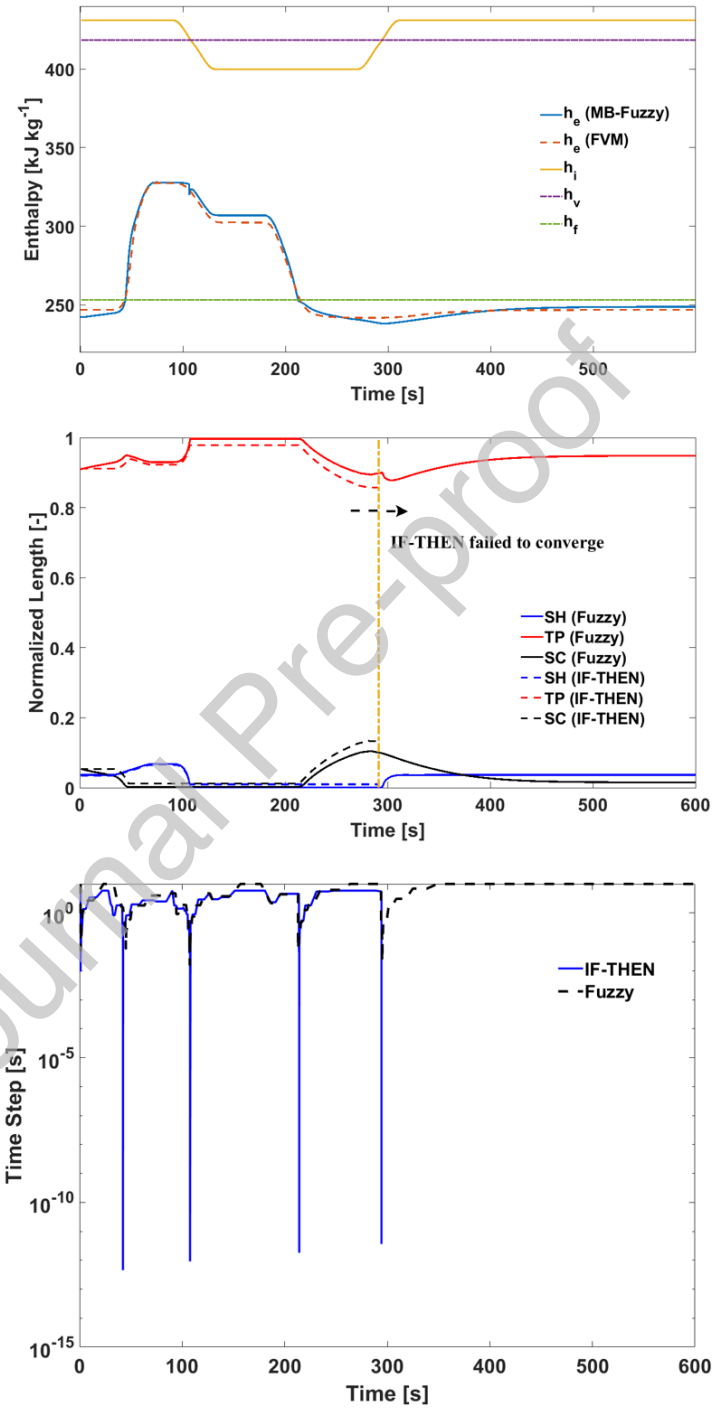

Figure 9: Test case simulation results

at around 100 sec (see Fig. 8), the SH region disappeared. The HX became TPSC at around 200 sec as the inlet mass flow rate decreased. Finally, the SH zone reappeared as the inlet enthalpy became higher than the saturated vapor enthalpy at around 300 sec.

The fuzzy MB model accurately predicted the moments when the subcooled liquid zone disappeared, at around 50 sec, and reappeared, at around 200 sec, in comparison with the FVM. The time errors are a few seconds. In addition, the outlet enthalpy profile of the presented model closely agreed with the FVM prediction with less than 5% relative errors for the entire simulation period despite the complex mode changes.

Comparisons of normalized zone lengths between the IF-THEN rule-based and fuzzy models illustrate that both models provided similar profiles for zone lengths for the first half of the simulation period. Although lengths for the subcooled liquid and superheat zones for the fuzzy MB model could be closer to zero than those for the IF-THEN model (see the dashed and solid lines for 100 - 200 sec), a smooth and reliable simulation of the fuzzy model was possible. This is because the weights associated with disappearing zones became small and reduced the influence of the singularity. Note that the IF-THEN model failed at around 300 second, when the inlet enthalpy was crossing the saturated vapor enthalpy to trigger the TPSC to SHTPSC switch. Since an enthalpy threshold was set, appearance of a superheated region would only be triggered when Eqn. (25) is satisfied. Then the numerical failure could have been caused by an inappropriate choice of threshold value. When the superheated region just reappears, its enthalpy is really close to saturated vapor enthalpy based on the linear profile, which makes the entries in the second line of the three-zone formulation matrix close to zero.

Integration time steps decided by the adaptive time step ode solver (the maximum integration step is set to a 10 sec) are compared: the value of a at t_1, for example, means that the next time step of evaluating differential equations after t_1 is $t_1 + a$. It can be seen that for the IF-THEN model very small time steps of around 10^{-12} sec, which is the default value for the smallest time step of the Simulink ode solvers, were chosen by the variable time step solver, ode15s, whenever the HX mode needed to be changed, i.e. at around 50, 100, 200 and 300 sec. This is necessary to treat discontinuities for ODE or DAE solvers as mentioned in the Section 2. The typical issue of halting and restarting the numerical integration can be clearly seen in the figure. On the other hand, the Fuzzy MB model doesn't exhibit the numerical reset although it still needs to reduce the time step near mode changes. The adjustment of the time step is because the Fuzzy model becomes stiff during the transitions and hence the adaptive time step ode solver had to reduce the time step until it met a prediction error tolerance (we used absolute error tolerance of 10^{-6} and relative error tolerance of 10^{-3}).

At the time of 300 sec when the IF-THEN model failed, the solver reduced the time step below 10^{-12} sec. The simulation failure implies that the ode solver could not reduce the error below the default error tolerances even with the smallest time step. In other words, the dynamics of the IF-THEN MB model are

too stiff to solve. The higher stiffness compared with the proposed MB model is attributed to the discontinuity associated with the IF-THEN rules. The simulation failure for an adaptive time step solver is an integrated effect of the MB formulation, switching algorithm, operating conditions, ode tolerances and smallest allowed time step. This makes general design of threshold parameters for IF-THEN based MB models challenging.

Parameter	**Unit**	**Value**
Initial conditions		
P	kPa	957.0
z_{SH}	-	0.035
z_{TP}	-	0.911
h_e	kJ kg^{-1}	242.5
T_{t1}	C	40.0
T_{t2}	C	36.0
T_{t3}	C	32.3
T_{w1}	C	36.0
T_{w2}	C	35.6
T_{w3}	C	30.1
Boundary conditions		
$\dot{m}_e$	kg s^{-1}	2.3
T_{wi}	C	29.8
$\dot{m}_w$	kg s^{-1}	16.8

Table 1: Numerical test case.

7. Reproducibility test under repeated mode changes

Following the approach introduced by McKinley and Alleyne (2008); Qiao et al. (2016), a reproducibiity test[1] of the final MB fuzzy model was conducted to see how reliably and smoothly a model behaves under repeated mode changes and to show the conservation of refrigerant mass during switches. A test scenario of a phase zone that disappears and appears at the outlet of the condenser used in the previous section was considered. Modes were repeatedly switched between SHTPSC and SHTP modes by imposing a sinusoidal signal on the refrigerant inlet mass flow rate. Other boundary conditions were held constant.

[1]In the references, the term of "stability test" was used. However, the terminology is confusing since "stability" is used in a different concept in controls. Therefore the term of "reproducibility test" is used in this paper to see how a model reliably and smoothly behaves and how simulation outcomes are reproducible under repeated input variations.

	Unit	Parameters
Initial conditions		SHTPSC↔SHTP
P	kPa	780.89
z_{SH}	-	0.0153
z_{TP}	-	0.9847
h_e	kJ/kg	260.01
T_{t1}	C	37.31
T_{t2}	C	30.32
T_{t3}	C	30.31
T_{w1}	C	30.42
T_{w2}	C	30.12
T_{w3}	C	27.34
Boundary conditions		
$\dot{m}_i$	kg/s	$1.254+0.5\sin(\pi t/150)$
h_i	kJ/kg	431.78
$\dot{m}_e$	kg/s	1.254
T_{wi}	C	27.34
$\dot{m}_w$	kg/s	16.7

Table 2: Reproducibility test cases.

Boundary conditions and initial conditions are described in Table 2. Simulations lasted for 2000 seconds and corresponding simulation results for subcooled zone length and refrigerant pressure are shown in Fig. 10 (a). As expected from the periodic boundary condition, phase zone length and refrigerant pressure also varied periodically. The conservation of mass was checked by calculating the total refrigerant mass (Fig. 10 (b) Simulated) within the heat exchanger and is compared with results from the integral form of refrigerant mass balance (Fig. 10 (b) Integral), with a maximum error of 4.3%. The smooth curves demonstrate the ability of the proposed schemes to switch between different model representations in a reliable manner, and refrigerant mass can be conserved in this process. The conservation of mass was addressed in the literature by ensuring a continuous mean void fraction (McKinley and Alleyne, 2008) or density (Cecchinato and Mancini, 2012) so that refrigerant charge calculation is consistent during switches. However, without complicating model representations, the conservation of mass can also be ensured by the proposed switching scheme, since state variables are inherently continuous, though errors can be introduced from property calculations.

8. Model Validation with Experimental Data

In this section, fuzzy MB HX models for an evaporator and condenser were integrated with models for a compressor, expansion valve (TXV) and a local controller to form a complete vapor compression cycle model. The integrated

model was compared with experimental data for a start-up transient of an R134a centrifugal chiller system. Refer to Bendapudi (2004) for detailed documentation of the test stand and component model descriptions. Fluid thermodynamic and transport properties were retrieved using Coolprop (Bell, Quoilin, Wronski and Lemort, 2013).

The start-up operation lasts for 1000 seconds. Fig. 11 shows variations of zone lengths determined using the MB model with fuzzy mode switching for both heat exchangers and provides a clear view of mode switches during the start-up period. When the system is turned on, refrigerant is pumped into the condenser very quickly, which increases the condensing pressure and simultaneously removes heat to the secondary fluid (water). This drives the leaving refrigerant of the condenser to condense to form the sub-cooled liquid zone (TPSC). On the other hand, as the refrigerant in the evaporator is depressurized due to the compressor start-up, it picks up heat from the chilled water forming a superheated vapor zone, which occured at around 50 sec, i.e. TPSH for the evaporator. This indicates that the condenser was SHTPSC at the time. After the mode switch of the evaporator, superheated vapor kept accumulating and during a very short period of time, refrigerant enthalpy increased to a point that the heat transfer between water and refrigerant balanced at around 90 sec. Unlike the condenser, the phase region length of evaporator kept varying after the normal operation mode (TPSH) was reached. This behavior was caused by variations in cycle boundary conditions as shown in Fig. 12. When the evaporator entering water temperature decreases, heat transfer between water and refrigerant is reduced, which drives the vapor phase zone length to decrease. When water inlet temperature increases, more heat is removed from water to refrigerant, so the vapor zone length increases accordingly.

Comparisons to the FVM HX based cycle model[2] and experimental data are presented in Fig. 13. Although the fuzzy MB model did not exactly match the dynamic behavior associated with the FVM model due to a fewer number of HX dynamics states, it certainly captures major dynamics of the chiller system associated with refrigerant pressures (a), exit enthalpies (b), and return water temperatures(c). The smooth transitions of the MB between different model representations demonstrate numerical reliability of the fuzzy switching algorithm. The MB model had a real time factor (Pangborn et al., 2015) of 0.128 as compared to a value for the FVM model of 0.898. With comparable accuracy, the MB executed approximately 7 times faster than the FVM model, which is consistent with observations in recent works by Bendapudi et al. (2008); Pangborn et al. (2015); Qiao et al. (2016); Rodriguez and Rasmussen (2017) .

[2]We refer to Bendapudi et al. (2008) for the FVM formulation. 15 control volumes were used for both condenser and evaporator

9. Conclusion and future work

In this paper, we present a novel heat exchanger moving boundary modeling approach that incorporates fuzzy modeling into the design of the moving boundary mode switching algorithm. It is believed that the approach is more computationally efficient than other moving boundary switching algorithms in the literature, since it eliminates discontinuities associated with IF-THEN rules. It is also intuitive and consistent. Furthermore, the proposed model has a much more compact and standard ode representation that makes it useful for control design and analysis.

Numerical tests to demonstrate accuracy and reliability of the proposed model are presented. An example case where an IF-THEN rule based moving boundary model resets the numerical integration process while the proposed model does not is provided. For the test of an integrated cycle model with the fuzzy HX models for a start-up transient of an R134a centrifugal chiller system, good agreement with a FVM based model and experimental data were achieved with about a factor of 7 reduction in computing time compared to the FVM model.

The design parameters for membership functions proposed in this paper are based on a parametric study. A more rigorous study will be performed in the future to investigate how the design of membership functions influences performance of a final fuzzy moving boundary model and to provide general guideline for implementation.

References

Bell, I.H., Quoilin, S., Wronski, J., Lemort, V., 2013. Coolprop: An open-source reference-quality thermophysical property library, in: ASME ORC 2nd International Seminar on ORC Power Systems.

Bendapudi, S., 2004. Development and evaluation of modeling approaches for transients in centrifugal chillers .

Bendapudi, S., Braun, J.E., Groll, E.A., 2008. A comparison of moving-boundary and finite-volume formulations for transients in centrifugal chillers. International journal of refrigeration 31, 1437–1452.

Bonilla, J., Dormido, S., Cellier, F.E., 2015. Switching moving boundary models for two-phase flow evaporators and condensers. Communications in nonlinear science and numerical simulation 20, 743–768.

Bradie, B., 2006. A friendly introduction to numerical analysis. Pearson Education India.

Brück, D., Elmqvist, H., Mattsson, S.E., Olsson, H., 2002. Dymola for multi-engineering modeling and simulation, in: Proceedings of modelica, Citeseer.

Casella, F., 2015. Simulation of large-scale models in modelica: State of the art and future perspectives, in: 11th International Modelica Conference, pp. 459–468.

Cecchinato, L., Mancini, F., 2012. An intrinsically mass conservative switched evaporator model adopting the moving-boundary method. International journal of refrigeration 35, 349–364.

Cellier, F.E., 1979. Combined continuous/discrete system simulation by use of digital computers: techniques and tools. Ph.D. thesis. ETH Zurich.

Cellier, F.E., Kofman, E., 2006. Continuous system simulation. Springer Science & Business Media.

Coddington, E.A., Levinson, N., 1955. Theory of ordinary differential equations. Tata McGraw-Hill Education.

Dahlquist, G., Björck, Å., et al., 1974. Numerical methods. Prentice Hall.

Fritzson, P., Aronsson, P., Pop, A., Lundvall, H., Nystrom, K., Saldamli, L., Broman, D., Sandholm, A., 2006. Openmodelica-a free open-source environment for system modeling, simulation, and teaching, in: 2006 IEEE Conference on Computer Aided Control System Design, 2006 IEEE International Conference on Control Applications, 2006 IEEE International Symposium on Intelligent Control, IEEE. pp. 1588–1595.

Galindo, J., Dolz, V., Royo-Pascual, L., Haller, R., Melis, J., 2016. Modeling and experimental validation of a volumetric expander suitable for waste heat recovery from an automotive internal combustion engine using an organic rankine cycle with ethanol. Energies 9, 279.

Grald, E.W., MacArthur, J.W., 1992. A moving-boundary formulation for modeling time-dependent two-phase flows. International Journal of Heat and Fluid Flow 13, 266–272.

He, X.D., Liu, S., Asada, H.H., Itoh, H., 1998. Multivariable control of vapor compression systems. HVAC&R Research 4, 205–230.

Kim, D., 2019. Moving boundary formulation. URL: https://github.com/kim1077/MBPaper_appendix.git.

Kim, D., Ziviani, D., Braun, J.E., Groll, E.A., 2017. A moving boundary modeling approach for heat exchangers with binary mixtures. Energy Procedia 129, 466–473.

Li, B., Alleyne, A.G., 2010. A dynamic model of a vapor compression cycle with shut-down and start-up operations. International Journal of refrigeration 33, 538–552.

Lundvall, H., Fritzson, P., Bachmann, B., 2008. Event handling in the openmodelica compiler and runtime system. Linköping University Electronic Press.

McKinley, T.L., Alleyne, A.G., 2008. An advanced nonlinear switched heat exchanger model for vapor compression cycles using the moving-boundary method. International Journal of Refrigeration 31, 1253–1264.

Mosterman, P.J., 1999. An overview of hybrid simulation phenomena and their support by simulation packages, in: International Workshop on Hybrid Systems: Computation and Control, Springer. pp. 165–177.

Munch Jensen, J., Tummescheit, H., 2002. Moving boundary models for dynamic simulations of two-phase flows, in: The second international modelica conference.

Pangborn, H., Alleyne, A.G., Wu, N., 2015. A comparison between finite volume and switched moving boundary approaches for dynamic vapor compression system modeling. International Journal of Refrigeration 53, 101–114.

Pettit, N., Willatzen, M., Ploug-Sørensen, L., 1998. A general dynamic simulation model for evaporators and condensers in refrigeration. part ii: simulation and control of an evaporator: Modèle général dynamique pour évaporateurs et condenseurs frigorifiques. partie ii: Simulation et régulation d'un évaporateur. International journal of refrigeration 21, 404–414.

Qiao, H., Laughman, C.R., Aute, V., Radermacher, R., 2016. An advanced switching moving boundary heat exchanger model with pressure drop. International Journal of Refrigeration 65, 154–171.

Quoilin, S., Desideri, A., Wronski, J., Bell, I., Lemort, V., 2014. Thermocycle: A modelica library for the simulation of thermodynamic systems, in: Proceedings of the 10th International Modelica Conference 2014.

Rasmussen, B.P., Alleyne, A.G., 2004. Control-oriented modeling of transcritical vapor compression systems. Journal of Dynamic Systems, Measurement, and Control 126, 54–64.

Rasmussen, B.P., Shenoy, B., 2012. Dynamic modeling for vapor compression systems—part ii: Simulation tutorial. HVAC&R Research 18, 956–973.

Rodriguez, E., Rasmussen, B., 2017. A comparison of modeling paradigms for dynamic evaporator simulations with variable fluid phases. Applied Thermal Engineering 112, 1326–1342.

Shampine, L.F., Reichelt, M.W., 1997. The matlab ode suite. SIAM journal on scientific computing 18, 1–22.

Shi, R., He, T., Peng, J., Zhang, Y., Zhuge, W., 2016. System design and control for waste heat recovery of automotive engines based on organic rankine cycle. Energy 102, 276–286.

Takagi, T., Sugeno, M., 1985. Fuzzy identification of systems and its applications to modeling and control. IEEE transactions on systems, man, and cybernetics , 116–132.

Wei, D., Lu, X., Lu, Z., Gu, J., 2008. Dynamic modeling and simulation of an organic rankine cycle (orc) system for waste heat recovery. Applied Thermal Engineering 28, 1216–1224.

Wetter, M., Zuo, W., Nouidui, T.S., Pang, X., 2014. Modelica buildings library. Journal of Building Performance Simulation 7, 253–270.

Willatzen, M., Pettit, N., Ploug-Sørensen, L., 1998. A general dynamic simulation model for evaporators and condensers in refrigeration. part i: moving-boundary formulation of two-phase flows with heat exchange: Modèle général dynamique pour évaporateurs et condenseurs frigorifiques. partic i: Formulation des conditions aux limites variables de flux biphasiques avec échange de chaleur. International Journal of refrigeration 21, 398–403.

Zhang, F., Yeddanapudi, M., Mosterman, P.J., 2008. Zero-crossing location and detection algorithms for hybrid system simulation. IFAC Proceedings Volumes 41, 7967–7972.

Zhang, W.J., Zhang, C.L., 2006. A generalized moving-boundary model for transient simulation of dry-expansion evaporators under larger disturbances. International Journal of refrigeration 29, 1119–1127.

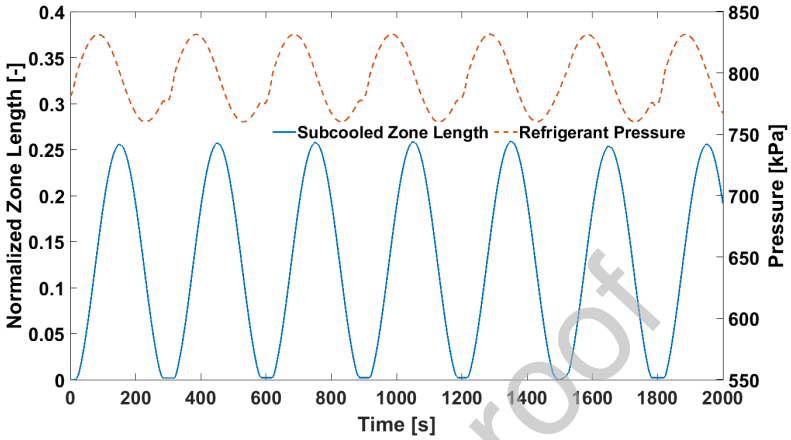

(a)

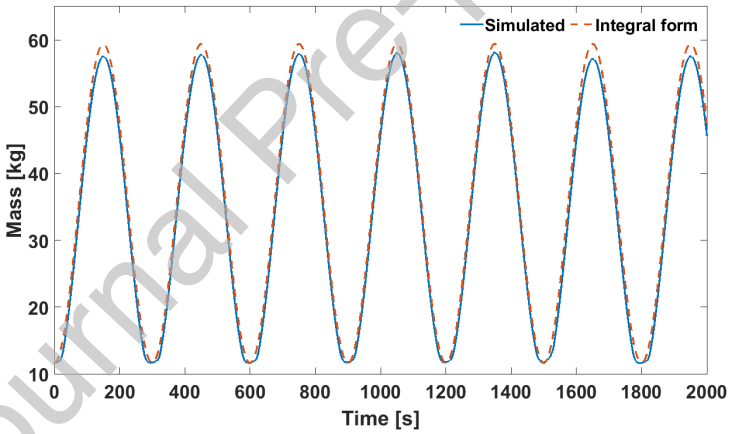

(b)

Figure 10: Reproducibility simulation results: (a) zone length and refrigerant pressure; (b) total refrigerant mass

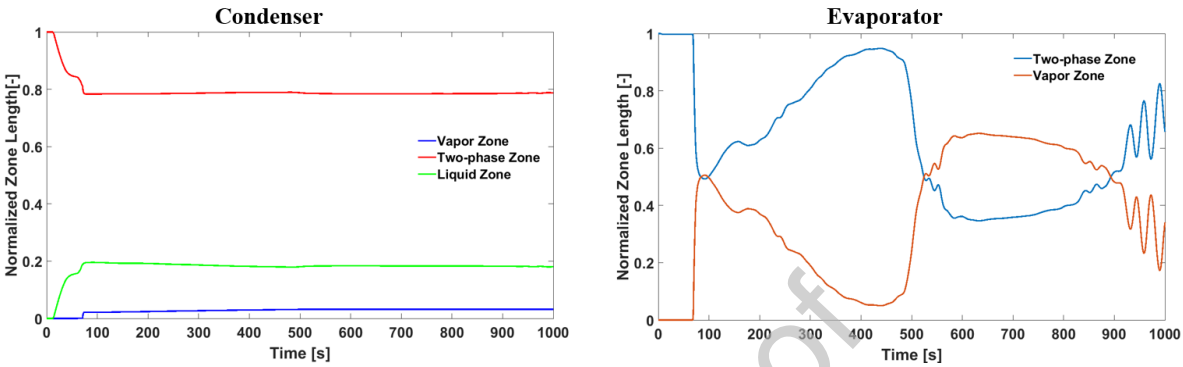

Figure 11: Variations in condenser and evaporator phase zone length

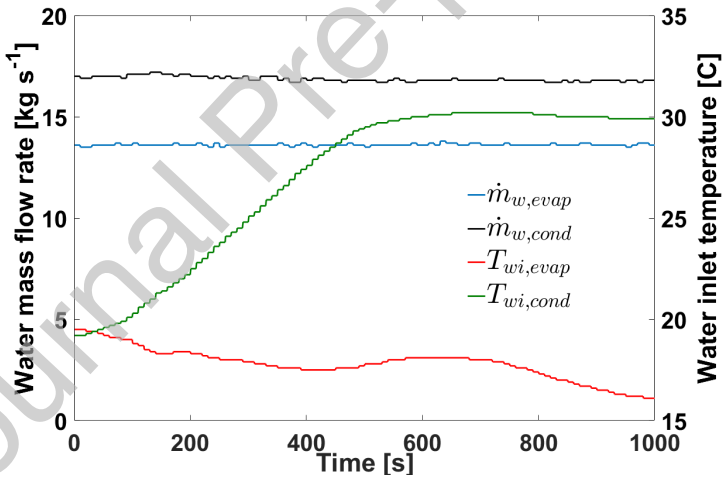

Figure 12: Cycle boundary conditions: heat exchangers water mass flow rate and inlet temperature

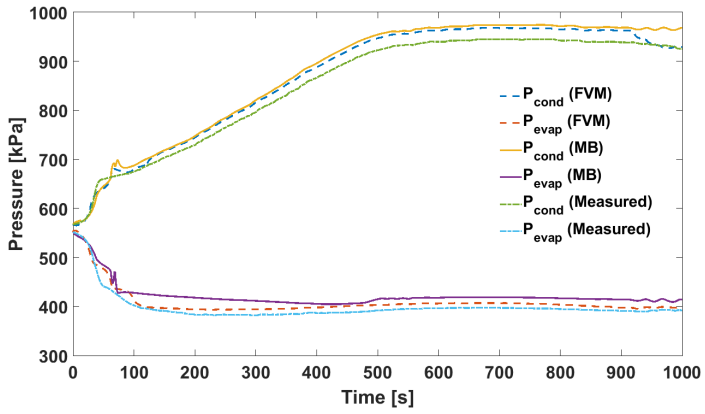

(a)

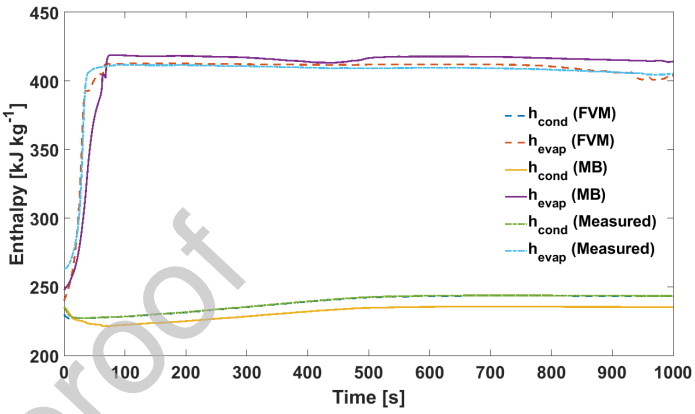

(b)

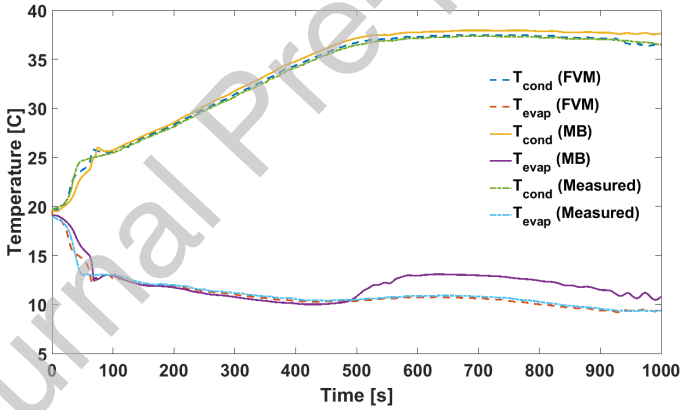

(c)

Figure 13: Start-up transients: (a) pressures; (b) exit enthalpies; (c) return water temperatures

Declaration of Competing Interest

The authors declare that they have no known competing financial interests or personal relationships that could have appeared to influence the work reported in this paper.